

Liouvillian exceptional points of any order in dissipative linear bosonic systems: Coherence functions and switching between \mathcal{PT} and anti- \mathcal{PT} symmetries

Ievgen I. Arkhipov,^{1,*} Adam Miranowicz,^{2,3,†} Fabrizio Minganti,^{3,‡} and Franco Nori^{3,4,§}

¹*Joint Laboratory of Optics of Palacký University and Institute of Physics of CAS, Faculty of Science, Palacký University, 17. listopadu 12, 771 46 Olomouc, Czech Republic*

²*Faculty of Physics, Adam Mickiewicz University, PL-61-614 Poznań, Poland*

³*Theoretical Quantum Physics Laboratory, RIKEN Cluster for Pioneering Research, Wako-shi, Saitama 351-0198, Japan*

⁴*Physics Department, The University of Michigan, Ann Arbor, Michigan 48109-1040, USA*

(Dated: September 15, 2020)

Usually, when investigating exceptional points (EPs) of an open Markovian bosonic system, one deals with spectral degeneracies of a non-Hermitian Hamiltonian (NHH), which can correctly describe the system dynamics only in the semiclassical regime. A recently proposed quantum Liouvillian framework [Minganti *et al.* *Phys. Rev. A* **100**, 062131 (2019)] enables the complete determination of the dynamical properties of such systems and their EPs (referred to as Liouvillian EPs, or LEPs) in the quantum regime by taking into account the effects of quantum jumps, which are ignored in the NHH formalism. Moreover, the symmetry and eigenfrequency spectrum of the NHH become a part of much larger Liouvillian eigenspace. As such, the EPs of an NHH form a subspace of the LEPs. Here we show that once an NHH of a dissipative linear bosonic system exhibits an EP of a certain finite order n , it immediately implies that the corresponding LEP can become of any higher order $m \geq n$, defined in the infinite Hilbert space. These higher-order LEPs can be identified by the coherence and spectral functions at the steady state. The coherence functions can offer a convenient tool to probe extreme system sensitivity to external perturbations in the vicinity of higher-order LEPs. As an example, we study a linear bosonic system of a bimodal cavity with incoherent mode coupling to reveal its higher-order LEPs; particularly, of second and third order via first- and second-order coherence functions, respectively. Accordingly, these LEPs can be additionally revealed by squared and cubic Lorentzian spectral lineshapes in the power and intensity-fluctuation spectra. Moreover, we demonstrate that these EPs can also be associated with spontaneous parity-time (\mathcal{PT}) and anti- \mathcal{PT} -symmetry breaking in the system studied. These symmetries can be switched in the output fields (the so-called supermodes) of an additional linear coupler with a properly chosen coupling strength. Thus, we show that the initial loss-loss dynamics for the supermodes can be equivalent to the balanced gain-loss evolution.

CONTENTS

I. Introduction	2	A. Non-Hermitian Hamiltonian exceptional second-order points and its anti- \mathcal{PT} - and \mathcal{PT} -symmetries	6
A. Exceptional points	2	1. Anti- \mathcal{PT} -symmetry and exceptional point of an effective non-Hermitian Hamiltonian	6
B. Liouvillian exceptional points	2	2. Switching to the \mathcal{PT} -symmetric modes	7
C. New results	2	3. Summary	7
D. Higher-order Liouvillian exceptional points in a bimodal cavity with incoherent mode coupling	3	B. Liouvillian exceptional points of higher orders	7
II. Liouvillian of a general dissipative linear bosonic system	3	1. LEP of second order and squared Lorentzian power spectra	8
III. Liouvillian exceptional points of any order in dissipative linear bosonic systems	4	2. Liouvillian exceptional point of third order and cubic Lorentzian intensity-fluctuation spectra	9
A. Higher-order correlation functions	4	3. Liouvillian exceptional point of third order explicitly defined from the higher-order field moments matrix	10
IV. Example of a bimodal cavity with incoherent mode coupling	6	V. Conclusions	11
		Acknowledgments	11
		A. Liouvillian \mathcal{L} for supermodes	12
		References	12

* ievgen.arkhipov@upol.cz

† miran@amu.edu.pl

‡ fabrizio.minganti@riken.jp

§ fnori@riken.jp

I. INTRODUCTION

A. Exceptional points

Exceptional points (EPs), which are exotic spectral degeneracies of non-Hermitian open systems, have attracted much interest in the last decades [1–3]. EPs arise when both eigenvalues and eigenfunctions of a non-Hermitian Hamiltonian (NHH) coalesce. Equivalently, an NHH, at its EPs, attains a Jordan form, i.e., it fails to be diagonalized. The advantages of EPs for applications remain a very active topic of research [4–18], in particular concerning the metrological advantages of EP sensitivity to external perturbations [1].

The concept of EPs was first introduced in connection with the perturbation theory of linear operators [19]. In physics, the notion of the EPs was further explored in connection with parity-time (\mathcal{PT}) symmetric quantum mechanics [20]. More recently, the concept of EPs has been investigated for general open quantum systems, where the interplay of incoherent drives and losses with coherent coupling can lead to the observation of an NHH spectral degeneracy [1, 2, 21, 22].

The presence of EPs in a system can produce a plethora of nontrivial phenomena. To name a few: unidirectional invisibility [23, 24], lasers with enhanced-mode selectivity [25, 26], low-power nonreciprocal light transmission [27–29], new types of thresholdless phonon lasers [30, 31], enhanced light-matter interactions [8, 9, 11], loss-induced lasing [32, 33], and even exceptional photon blockade [34]. These exotic phenomena have been observed in different experimental platforms, based on electronics [35], optomechanics [30, 36–38], acoustics [39, 40], plasmonics [41], and metamaterials [42]. Moreover, the concept of EPs has been successfully exploited in describing dynamical quantum phase transitions and topological phases of condensed matter in open quantum systems [43–51], and its relation to nonclassicality in photonic systems [52, 53].

B. Liouvillian exceptional points

Recently, an extension of the concept of EPs from an NHH formalism to that based on the quantum Liouvillian has been proposed [54]. Indeed, the inclusion of quantum jumps can have a profound effect on the systems dynamics and its spectra [54–59]. Moreover, the eigenspectrum of an NHH becomes a part of much larger eigenspace of a Liouvillian, meaning that EPs of an NHH, which from hereon we denote as HEPs, become a part of Liouvillian EPs which are usually denoted as LEPs. As such, the quantum Liouvillian formalism appears to be a natural choice to study EPs of an open quantum system. Nonetheless, in some systems, e.g., in a double-quantum-dot circuit QED setup [60], the NHH can capture nontrivial system dynamics, which is “invisible” using the corresponding Liouvillian.

At the same time, very recent works have already shown that switching to the Liouvillian framework allows to reveal nontrivial phenomena, which cannot be observed within the NHH formalism. These include the existence of higher-order LEPs compared with lower-order HEPs [56, 61], or the possibility to detect nontrivial EPs by using a hybrid Liouvillian formalism [57]. Moreover, \mathcal{PT} -symmetry has been reformulated within a Liouvillian framework [55, 59, 62].

C. New results

In this work, we demonstrate that for a dissipative linear bosonic system, whose effective NHH exhibits a HEP of any finite order n , determined by first-order field moments, the corresponding LEPs can become at least of order $m \geq 2k(n-1) + 1$, for $k = \frac{1}{2}, 1, 2, 3, \dots$, determined by higher-order field moments, accordingly. These m th-order LEPs can be identified by the $(m-1)$ st-order coherence and spectral response functions in the steady state of the system. Because the steady state of such systems is a thermal state, by exploiting the well-known moments theorem [63], the coherence functions of arbitrary order can be completely determined by the first-order coherence function, i.e., by its products. As such, by identifying a HEP with the first-order coherence function [56], one then can identify higher-order LEPs by means of the corresponding higher-order coherence functions. Importantly, the coherence functions can only be determined by the *Liouvillian eigenspace*.

We stress that when considering an NHH in an infinite-dimensional system, one can also determine infinitely-high-order HEPs related to high-order moments of the fields [64, 65]. Nevertheless, NHHs fail to include quantum jumps and thermal noise. A striking example of this fact comes from an effective Hamiltonian which commutes with the total photon number operator. While at the NHH level this implies that manifolds with different numbers of excitations cannot interact, the quantum jumps of the Liouvillian can still mix states with different photon numbers. These different properties of the NHH and the corresponding Liouvillian imply that also their eigenstates are different [54, 56]. As a result, the equations of motion for second- or higher-order quantum field moments differ for the Liouvillian and NHH formalisms, indicating their distinguishable spectral properties. Hence, the analyses of higher-order HEPs resulting from higher-order moments are predictive only in the semiclassical regime, when the operators can be treated as c -numbers. In other words, *a correct description of spectral properties of a quantum system via its higher-order field moments needs to rely exclusively on the Liouvillian eigenspectrum*.

D. Higher-order Liouvillian exceptional points in a bimodal cavity with incoherent mode coupling

As an example of the above general result, we study a bosonic system of a bimodal cavity with incoherent mode coupling to reveal its higher-order Liouvillian EPs. The incoherent mode interaction can be encoded by the off-diagonal elements of the damping matrix in the quantum Liouvillian [66, 67]. These off-diagonal damping coefficients naturally appear in the microscopic theory of overlapping modes in open resonators [66] and chaotic two-mode lasers [68], where a strong interaction with the surrounding environment can induce a mode overlapping in the multimode cavities. Moreover, these theories have proved useful in explaining the Petermann excess noise factor in random lasers [68, 69] and describing intensity-fluctuation spectra in bimodal cavities coupled to quantum emitters [70, 71]. Interestingly, one of the first experimental observations of the intermode coupling in a bimodal cavity due to the interaction with surrounding screening fields, induced by a conducting sample located near the cavity, was already reported a few decades ago in Ref. [72], where microwave Hall measurements were performed. Incoherent mode coupling can be produced in various ways. These have been already realized, e.g., in anti- \mathcal{PT} -symmetrical *classical* systems, which include: nonlinear Brillouin scattering in a single microcavity [73], two passive waveguides, separated by a metallic film [74], countermoving media with heat exchange [75] or resistively coupled electric resonators [76]; and, in quantum systems, through a coherent transport of flying atoms [77]. Nevertheless, in all these works, when studying EPs, a phenomenological approach has been utilized based exclusively on effective NHHs, thus ignoring quantum-jump effects.

In particular, we analyze second and third-order LEPs of such systems arising from a HEP of second order by calculating the first- and second-order coherence functions, respectively. Also, we calculate the corresponding power and intensity-fluctuation spectra to reveal their squared and cubic Lorentzian expressions, accordingly. We also reveal the anti- \mathcal{PT} - and \mathcal{PT} -symmetries of the NHH, which connect the presence of LEPs with spontaneous breaking of such symmetries in a bimodal cavity with incoherent mode coupling. We show the possibility of switching between the \mathcal{PT} and anti- \mathcal{PT} symmetries of bosonic linear systems, like linearly-coupled harmonic cavities. This switching can simply be realized by applying a tunable linear coupler (e.g., a tunable beam splitter in optical implementations) to a two-mode output field of the system. Moreover, our analysis of such two-mode systems reveals that for an LEP of odd order ($2k+1$), the system enhanced sensitivity to external perturbations ϵ scales at most as $\epsilon^{\frac{1}{2k}}$.

We stress that the discussed \mathcal{PT} and anti- \mathcal{PT} symmetries in our study are exclusively related to the symmetries of the NHH, which plays a central role in our work. However, we note that the recent studies in

Refs. [55, 59, 62] have already addressed the properties of \mathcal{PT} -symmetry of the whole Liouvillian. Since here we focus on dissipative systems, the whole Liouvillian does not possess the \mathcal{PT} -symmetry in the sense of, e.g., Ref. [20]. Nonetheless, the studied Liouvillian, for a two-site system, is *passively* \mathcal{PT} -symmetric. In other words, it acquires the \mathcal{PT} -symmetry in a reference frame with global decay [55, 59]; that is, after applying an appropriate gauge transformations.

Let us recall now the meaning of the \mathcal{PT} and anti- \mathcal{PT} symmetries of the NHH. In general, a system described by a Hamiltonian \hat{H} exhibits the \mathcal{PT} (anti- \mathcal{PT}) symmetry if \hat{H} commutes (anticommutes) with the \mathcal{PT} operator. Here the parity operator \mathcal{P} transforms a position operator \hat{x} to $-\hat{x}$ and a momentum operator \hat{p} to $-\hat{p}$, while the time reversal operator \mathcal{T} transforms $\hat{x} \rightarrow \hat{x}$ and $\hat{p} \rightarrow -\hat{p}$, and performs complex conjugation $i \rightarrow -i$.

This paper is organized as follows. In Sec. II, we briefly introduce a general Liouvillian for a dissipative multimode bosonic system. In Sec. III, we present our main result, namely that any HEP of a finite order implies the infinite order of the corresponding LEP. As an example, we study higher-order LEPs in a bimodal cavity with incoherent mode coupling in Sec. IV. In particular, we analyze second and third-order LEPs by means of the first and second-order coherence functions, respectively, along with the power and intensity-fluctuation spectra to reveal their squared and cubic Lorentzian lineshapes at the corresponding LEPs. We also demonstrate that EPs in such systems can be directly associated with \mathcal{PT} and anti- \mathcal{PT} -symmetry breaking. Conclusions are drawn in Sec. V.

II. LIOUVILLIAN OF A GENERAL DISSIPATIVE LINEAR BOSONIC SYSTEM

The dynamics of a density matrix $\hat{\rho}$ describing a quantum system interacting with its environment is governed by a completely positive trace-preserving (CPTP) map. In the limit of weak Markovian time-independent interactions, such a CPTP map is known as the Liouvillian superoperator \mathcal{L} whose action is described by the master equation:

$$\frac{d}{dt}\hat{\rho}(t) = \mathcal{L}\hat{\rho}(t). \quad (1)$$

For an N -mode open linear coupled bosonic system interacting with thermal environment, the Liouvillian has the following general Gorini-Kossakowski-Sudarshan-Lindblad form ($\hbar = 1$) [66, 67]:

$$\begin{aligned} \mathcal{L}\hat{\rho} = & -i \left[\hat{H}, \hat{\rho} \right] + \frac{n_{\text{th}} + 1}{2} \sum_{j,k} \gamma_{jk} \mathcal{D} \left[\hat{a}_j, \hat{a}_k^\dagger \right] \hat{\rho} \\ & + \frac{n_{\text{th}}}{2} \sum_{j,k} \gamma_{jk} \mathcal{D} \left[\hat{a}_j^\dagger, \hat{a}_k \right] \hat{\rho}, \end{aligned} \quad (2)$$

where \hat{H} is a Hermitian Hamiltonian, and the general Lindblad dissipators are

$$\mathcal{D} \left[\hat{\Gamma}_j, \hat{\Gamma}_k^\dagger \right] \hat{\rho} = 2\hat{\Gamma}_j \hat{\rho} \hat{\Gamma}_k^\dagger - \hat{\Gamma}_k^\dagger \hat{\Gamma}_j \hat{\rho} - \hat{\rho} \hat{\Gamma}_k^\dagger \hat{\Gamma}_j. \quad (3)$$

In Eq. (2), \hat{a}_j (\hat{a}_j^\dagger) is the annihilation (creation) operator of mode j ; the diagonal damping coefficients γ_{kk} denote the inner k th mode decay rate, while the off-diagonal coefficients γ_{jk} denote the *incoherent* coupling between modes j and k , due to the interaction of both modes with the environment [66]. Without loss of generality, we assume that the thermal photon number n_{th} is constant throughout the spectral range of a system. The Liouvillian \mathcal{L} can also be recast in the following form

$$\begin{aligned} \mathcal{L}\hat{\rho} = & -i \left(\hat{H}_{\text{eff}} \hat{\rho} - \hat{\rho} \hat{H}_{\text{eff}}^\dagger \right) + \frac{n_{\text{th}} + 1}{2} \sum_{j,k} \hat{a}_j \hat{\rho} \hat{a}_k^\dagger \\ & + \frac{n_{\text{th}}}{2} \sum_{j,k} \hat{a}_j^\dagger \hat{\rho} \hat{a}_k, \end{aligned} \quad (4)$$

where \hat{H}_{eff} is an effective NHH given by:

$$\hat{H}_{\text{eff}} = \hat{H} - \frac{i}{2} \sum_{j,k} \gamma_{jk} \hat{a}_j^\dagger \hat{a}_k. \quad (5)$$

Note that the term $\left(\hat{H}_{\text{eff}} \hat{\rho} - \hat{\rho} \hat{H}_{\text{eff}}^\dagger \right)$ in Eq. (4) can be interpreted as a generalized commutator. Moreover, this NHH is not Hermitian, i.e., $\hat{H}_{\text{eff}} \neq \hat{H}_{\text{eff}}^\dagger$. Additionally, the Hermitian Hamiltonian in Eq. (5) for a linear coupled system can be written in a general form

$$\hat{H} = \sum_k \omega_k \hat{a}_k^\dagger \hat{a}_k + \sum_{j < k} \left(\chi_{jk} \hat{a}_j^\dagger \hat{a}_k + \text{H.c.} \right), \quad (6)$$

where ω_k is a bare frequency of the mode k , and χ_{jk} is the coherent coupling coefficient between modes j and k .

III. LIOUVILLIAN EXCEPTIONAL POINTS OF ANY ORDER IN DISSIPATIVE LINEAR BOSONIC SYSTEMS

In a recent work [61], it has been shown that if a NHH has an EP of n th order, then it implies that a LEP is at least of order $(2n-1)$. Below, we demonstrate in a simple manner that if an NHH of a linear bosonic system has an EP of any order $n \geq 2$, determined by the first-order field moments, then this EP actually implies an infinite order for the LEP, which, accordingly, is determined by higher-order field moments, and, thus, can be identified by higher-order coherence functions.

To show this general result, let us first start describing the time dynamics of the system field averages $\langle \hat{a}_j(t) \rangle$. Note that we are working exclusively in the Schrödinger picture; thus, for simplicity, we put the time parameter t inside triangular brackets. After applying the formula for the time derivative of the field averages

$$\frac{d}{dt} \langle \hat{a}_j(t) \rangle = \text{Tr} \left[\hat{a}_j \frac{d}{dt} \hat{\rho}(t) \right], \quad (7)$$

and using Eqs. (1), (2), and (7), one obtains a linear system

$$v(t) = \exp(-i\hat{H}_{\text{eff}}t)v(0) \quad (8)$$

where $v(t) = [\langle \hat{a}_1(t) \rangle, \langle \hat{a}_2(t) \rangle, \dots, \langle \hat{a}_N(t) \rangle]^T$ is a vector of the operator averages, and \hat{H}_{eff} is a matrix form of the effective NHH in Eq. (5).

Hence, the dynamics of the annihilation operators imposed by the Liouvillian \mathcal{L} can be fully determined by the eigenspectrum of the effective NHH \hat{H}_{eff} . As a result, the appearance of an EP in the NHH spectrum, immediately implies the emergence of the same EP in the Liouvillian spectrum [56]. Namely, the relationship between the eigenfrequencies (eigenvalues): $\nu \equiv \nu_{\text{NHH}}$ of the NHH and $\lambda \equiv \lambda_{\mathcal{L}}$ of the Liouvillian, which define the time dynamics of the fields in Eq. (8), bear a simple form [56]:

$$\lambda_{\mathcal{L}} = -i\nu_{\text{NHH}}. \quad (9)$$

Therefore, the coalescence of the eigenvalues ν_{NHH} of the NHH, along with its eigenstates, indicates the coalescence of the eigenvalues $\lambda_{\mathcal{L}}$ and the corresponding eigenstates of the Liouvillian. These eigenvalues merging cause the NHH to acquire a nondiagonal Jordan form; which is, then, reflected in the nonexponential character of the time evolution of the cavity fields, according to Eq. (8). Moreover, the symmetry shared by the NHH becomes, in general, a local symmetry of the Liouvillian. The latter stems from the fact that the Liouvillian does not necessarily have the global symmetries of the NHH. We stress that the above conclusion of the coincidence of EPs of the NHH and Liouvillian is valid for any linear quadratic NHH in Eq. (5), with its coherent part given in Eq. (6). Moreover, the damping coefficients in the Lindblad dissipators in Eq. (3) may attain any form, e.g., similar to that of the Scully-Lamb laser model [56], as long as the system remains linear, i.e., dissipative.

A. Higher-order correlation functions

The exact equivalence between the effective Hamiltonian and Liouvillian predictions of the spectral properties of the system holds true only for the dynamics of the annihilation operators. For example, higher-power field averages $\langle \hat{a}_j^\dagger m \hat{a}_j^n(t) \rangle$ would be affected by the presence of quantum jumps in a nontrivial way. Nevertheless, from the presence of a first-order HEP one we can deduce the properties of higher-order correlation functions, which, for linear systems, are determined by the higher-order field moments. Indeed, this function, at the steady state, can be calculated according to the formula:

$$g_{j,ss}^{(1)}(\tau) = \frac{\langle \hat{a}_j^\dagger(0) \hat{a}_j(\tau) \rangle_{ss}}{\langle \hat{a}_j^\dagger(0) \hat{a}_j(0) \rangle_{ss}}, \quad j = 1, \dots, N, \quad (10)$$

where $\langle \hat{a}_j^\dagger(0) \hat{a}_j(\tau) \rangle_{ss}$ is a two-time correlation function (TTCF) for the mode j at the steady state. The TTCF,

in turn, can be easily computed by exploiting the quantum regression theorem [63, 78]. Namely, by solving the equations of motion for the field averages $\langle \hat{a}(\tau) \rangle$ in Eq. (8), one can immediately obtain $\langle \hat{a}^\dagger(0)\hat{a}(\tau) \rangle$. The TTCF for, e.g., the field \hat{a}_1 reads as [56]:

$$f_j(\tau) = \exp(-i\hat{H}_{\text{eff}}\tau)f_j(0), \quad (11)$$

where $f(\tau) = [\langle \hat{a}_j^\dagger(0)\hat{a}_1(\tau) \rangle_{\text{ss}}, \dots, \langle \hat{a}_j^\dagger(0)\hat{a}_N(\tau) \rangle_{\text{ss}}]^T$ is a vector of TTCFs for the mode j .

In other words, the dynamics and symmetry of the equations of motion for the coherence function $g^{(1)}(\tau)$ is determined by the same effective NHH. Again, at the HEP of n th order, the NHH obtains a Jordan form. As a result, and according to Eq. (11), the coherence function $g^{(1)}(\tau)$, regardless of the mode j , attains a nonexponential form, with the highest power degree in τ , as follows:

$$g_{\text{ss}}^{(1)}(\tau) \sim \tau^{n-1} \exp(-i\nu_{\text{HEP}}\tau), \quad (12)$$

where ν_{HEP} , with imaginary part $\text{Im}(\nu_{\text{HEP}}) < 0$, is a complex eigenvalue of the NHH at an HEP of n th order.

The steady state of the considered linear systems with the Liouvillian \mathcal{L} , given in Eq. (2), along with the Hamiltonian in Eq. (6), is a thermal state. As a result, the higher-order coherence functions $g_{\text{ss}}^{(k)}(\tau)$, $k \in \mathbb{N}$, at the steady state, are completely determined by the first-order coherence function $g_{\text{ss}}^{(1)}(\tau)$, according to the moments theorem [63].

The higher-order coherence functions $g_{j,\text{ss}}^{(2k)}(\tau)$, based on the TTCFs, are found as

$$g_{j,\text{ss}}^{(2k)}(\tau) = \frac{\langle \hat{a}_j^{\dagger k}(0)\hat{a}_j^{\dagger k}(\tau)\hat{a}_j^k(\tau)\hat{a}_j^k(0) \rangle_{\text{ss}}}{\langle \hat{a}_j^\dagger(0)\hat{a}_j(0) \rangle_{\text{ss}}^{2k}}. \quad (13)$$

The form of the coherence function $g_{j,\text{ss}}^{(2k)}(\tau)$ in Eq. (13) ensures that at the n th-order HEP, the $(2k)$ th-order coherence function at the steady state contains the following term with the highest power degree in τ :

$$g_{\text{ss}}^{(2k)}(\tau) \sim \tau^{2k(n-1)} \exp\left[2k\text{Im}(\nu_{\text{HEP}})\tau\right], \quad (14)$$

For instance, the second-order coherence function $g_{\text{ss}}^{(2)}(\tau)$ for the thermal light takes a simple form

$$g_{\text{ss}}^{(2)}(\tau) = 1 + \left|g_{\text{ss}}^{(1)}(\tau)\right|^2 \sim \tau^{2n-2} \exp\left[2\text{Im}(\nu_{\text{HEP}})\tau\right]. \quad (15)$$

The coherence function $g_{\text{ss}}^{(2k)}(\tau)$ is solely defined by the Liouvillian eigenspectrum; thus, at the HEP of the n th order, this function implies the coalescence of $[2k(n-1)+1]$ Liouvillian eigenvectors. This means that the LEP becomes at least of the order $[2k(n-1)+1]$. Moreover, because of the infinite-dimensional Hilbert space of a general bosonic system, the coherence function can be, thus, of infinite order. Thus, a HEP would simply imply the existence of the LEP of *infinite* order. In other words,

the order of an LEP is only limited by the maximal possible number of photons in a system, i.e., the maximal size of its Hilbert space.

To shed more light on this direct connection between the higher-order LEPs and higher-order coherence functions, let us recall the general formula for the TTCFs for the steady state, which is used in the definition of the coherence function:

$$\langle \hat{O}_1(0)\hat{O}_2(\tau)\hat{O}_3(0) \rangle_{\text{ss}} = \text{Tr} \left\{ \hat{O}_2(0)e^{\mathcal{L}\tau} \left[\hat{O}_3(0)\hat{\rho}_{\text{ss}}\hat{O}_1(0) \right] \right\}, \quad (16)$$

where \hat{O}_j are some system operators. The operator $\hat{O}_3\hat{\rho}_{\text{ss}}\hat{O}_1$, in Eq. (16), leads the steady state $\hat{\rho}_{\text{ss}}$ into the new state, which becomes a decomposition of the Liouvillian eigenmatrices $\hat{\rho}_i$, i.e.,

$$\hat{O}_3\hat{\rho}_{\text{ss}}\hat{O}_1 = \sum_i c_i \hat{\rho}_i. \quad (17)$$

By recalling the linearity of the trace, we have

$$\langle \hat{O}_1(0)\hat{O}_2(\tau)\hat{O}_3(0) \rangle_{\text{ss}} = \sum_i c_i \text{Tr} \left\{ \hat{O}_2(0)e^{\mathcal{L}\tau} [\hat{\rho}_i] \right\}. \quad (18)$$

In the presence of an LEP, one finally has

$$\langle \hat{O}_1(0)\hat{O}_2(\tau)\hat{O}_3(0) \rangle_{\text{ss}} = \sum_i c_i \tau^{n_i} e^{\lambda_i \tau} \text{Tr} \left\{ \hat{O}_2(0)\hat{\rho}_i \right\}, \quad (19)$$

where n_i is the degree of the degeneracy of the LEP associated with the eigenmatrix $\hat{\rho}_i$ (see also Ref. [56] for more details). Moreover, the eigenmatrices $\hat{\rho}_i$ correspond to various powers of the boson operators of the fields [79], which means that this is the eigenspace of higher-order field moments that is identified by the TTCFs. In our particular case, $\hat{O}_1 = \hat{a}^{\dagger k}$, $\hat{O}_2 = \hat{a}^{\dagger k}\hat{a}^k$, and $\hat{O}_3 = \hat{a}^k$. Note that TTCFs, in Eq. (16), can be applied to any moments of the field, i.e., not necessarily to the Hermitian moments $O_2(\tau) = \hat{a}^{\dagger k}(\tau)\hat{a}^k(\tau)$. As such, it is possible to reveal an arbitrary order m of a LEP, apart from that identified by the coherence function $g_{\text{ss}}^{(2k)}(\tau)$.

Experimentally, the spectral properties of dissipative systems have been measured, in particular regarding the closure of the Liouvillian gap occurring in dissipative phase transitions [80]. In particular, in Ref. [81] the two-time correlation function has been used to prove the occurrence of the first-order phase transition of a semiconductor micropillar, as predicted in Refs. [82, 83]. Moreover, optical hysteresis properties have been used in Ref. [84] to prove the emergence of a critical slowing-down effect. Similarly, in Ref. [85] the emergence of a slow timescale in a one-dimensional superconductor chain has been used to pinpoint the precursors of a dissipative phase transition in a driven-dissipative Bose-Hubbard model [86, 87].

We conclude that observing LEPs using the first- and second-order correlation functions is within the experimental reach of current techniques. For instance, an n th-order HEP would imply the possibility to measure a LEP

at least of order $(2n - 1)$ [61] by means of the coherence function $g_{ss}^{(2)}(\tau)$. We note that, however, to access higher-order LEPs using higher-order coherence functions could be much more challenging. Indeed, $g_{ss}^{(2k)}(\tau)$ decays much faster than $g_{ss}^{(2)}(\tau)$ [c.f. Eq. (14)], thus reducing the visibility of its nonexponential behavior.

IV. EXAMPLE OF A BIMODAL CAVITY WITH INCOHERENT MODE COUPLING

In this section, we study higher-order LEPs in a bimodal cavity with incoherent mode coupling. In particular, we analyze second- and third-order LEPs arising from a HEP of the second order by calculating first- and second-order coherence functions, respectively. Also, we calculate the corresponding power and intensity-fluctuation spectra to reveal their squared and cubic Lorentzian lineshapes, accordingly. Additionally, we reveal the anti- \mathcal{PT} - and \mathcal{PT} -symmetries of the NHH, which connect the presence of the LEPs with spontaneous breaking of such symmetries in the system.

A. Non-Hermitian Hamiltonian exceptional second-order points and its anti- \mathcal{PT} - and \mathcal{PT} -symmetries

1. Anti- \mathcal{PT} -symmetry and exceptional point of an effective non-Hermitian Hamiltonian

The dynamics of a density matrix $\hat{\rho}$ of a bimodal cavity with incoherent mode coupling is described by the Liouvillian in Eq. (2) with the free coherent Hamiltonian of the form

$$\hat{H} = \sum_{k=1,2} \omega_k \hat{a}_k^\dagger \hat{a}_k. \quad (20)$$

For simplicity, we further assume that the damping matrix γ_{jk} is symmetric, i.e., $\gamma_{21} = \gamma_{12}$, and the inner mode decaying rates are the same, i.e., $\gamma_{11} = \gamma_{22} = \gamma$.

By working in the rotating reference frame with the central frequency $\bar{\omega} = (\omega_1 + \omega_2)/2$, the effective NHH, given in Eq. (5), attains the form

$$\hat{H}_{\text{eff}} = \frac{1}{2} \begin{pmatrix} \Delta - i\gamma & -i\gamma_{12} \\ -i\gamma_{12} & -\Delta - i\gamma \end{pmatrix}, \quad (21)$$

where $\Delta = (\omega_1 - \omega_2)$ is a cavity resonance difference.

This NHH is anti- \mathcal{PT} -symmetric, meaning that its anticommutator with a \mathcal{PT} operator is zero:

$$\mathcal{PT} \hat{H}_{\text{eff}} (\mathcal{PT})^{-1} = -\hat{H}_{\text{eff}}. \quad (22)$$

The action of the time-reversal operator \mathcal{T} on the NHH \hat{H}_{eff} is equivalent to

$$\mathcal{T} \hat{H}_{\text{eff}} \mathcal{T}^{-1} = \hat{H}_{\text{eff}}^*,$$

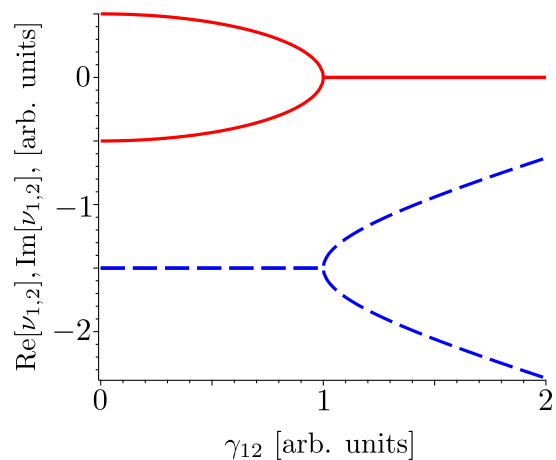


FIG. 1. Real (red solid curves) and imaginary (blue dashed curves) parts of the eigenfrequencies ν_1 and ν_2 of the effective NHH \hat{H}_{eff} versus the incoherent coupling rate γ_{12} . These eigenfrequencies constitute a subset of the eigenfrequencies of the Liouvillian \mathcal{L} , of a bimodal cavity according to Eq. (23). The chosen system parameters are: the frequencies of the modes $\omega_2 = -\omega_1 = 0.5$ [arbitrary units]; the cavity losses for both modes \hat{a}_1 and \hat{a}_2 are $\gamma = 3$ [arb. units]. The system experiences a spectral-phase transition at the EP $\gamma_{12}^{\text{EP}1}$, according to Eq. (26), due to the interplay between the mode frequency difference Δ and the incoherent mode coupling γ_{12} .

where the asterisk indicates the complex conjugation. And the parity operator \mathcal{P} is equivalent to the Pauli $\hat{\sigma}_x$ matrix. The presence of the incoherent mode coupling rate γ_{12} , thus, induces the anti- \mathcal{PT} -symmetry in the evolution of the field averages.

The eigenspectrum of the NHH gives two possible eigenvalues:

$$\nu_{1,2} = -i\frac{\gamma}{2} \pm \frac{i}{2}D, \quad (23)$$

where

$$D = \sqrt{\gamma_{12}^2 - \Delta^2}. \quad (24)$$

The unnormalized eigenvectors of the NHH, then, can be easily found as

$$\psi_{1,2} \equiv \begin{pmatrix} i\gamma_{12} \\ \Delta \mp iD \end{pmatrix}. \quad (25)$$

From Eqs. (23) and (25) it follows that the NHH \hat{H}_{eff} , and, thus, the Liouvillian, attain an EP

$$\gamma_{12}^{\text{EP}} = |\Delta| = |\omega_1 - \omega_2|. \quad (26)$$

At this EP, the NHH experiences a spectral-phase transition, associated with anti- \mathcal{PT} -symmetry breaking. Meaning that cavity fields in Eq. (8) can exist in two different spectral phases.

We plot the eigenfrequencies ν_1 and ν_2 in Fig. 1. When $\gamma_{12} > \Delta$, i.e., the NHH eigenvalues $\nu_{1,2}$ both become

purely imaginary, the NHH eigenstates ψ_1 and ψ_2 are in the exact anti- \mathcal{PT} symmetric phase. That is, the eigenmodes ψ_1 and ψ_2 become asymmetric, the former attaining an effective gain and the latter acquiring additional losses proportional to the parameter $|D|$ [see Eq. (23)]. Contrary to this, when $\gamma_{12} < \Delta$, the eigenvalues are no longer purely imaginary, and the eigenstates of the NHH are in the broken anti- \mathcal{PT} -symmetric phase. In this case, the two modes are spectrally separated, and this mode splitting can be defined by the real-valued parameter $|D|$ given in Eq. (23).

2. Switching to the \mathcal{PT} -symmetric modes

By appropriate unitary transformations, the effective NHH in Eq. (21) can be recast into a form, where it acquires a \mathcal{PT} -like symmetry, namely, *passive* \mathcal{PT} -symmetry. For this, we can introduce the general *combined modes* (often referred to as *supermodes*) \hat{c}_1 and \hat{c}_2 (see, e.g., [70, 88]), defined via the rotation

$$\begin{pmatrix} \hat{c}_1 \\ \hat{c}_2 \end{pmatrix} = \begin{pmatrix} \cos \theta & -\sin \theta \\ \sin \theta & \cos \theta \end{pmatrix} \begin{pmatrix} \hat{a}_1 \\ \hat{a}_2 \end{pmatrix}, \quad (27)$$

where θ is an appropriate angle. This transformation of \hat{a}_1 and \hat{a}_2 to the supermodes \hat{c}_1 and \hat{c}_2 can simply be realized with a tunable linear coupler. In case of optical implementations of our system, this coupler can be realized by a single tunable beam splitter or, in more refined implementations, by a Mach-Zehnder interferometer [89].

For the case under consideration, i.e., $\gamma_{12} = \gamma_{21}$, the Lindblad master equation, given in Eq. (2), can be put in the diagonal form of the damping matrix γ_{jk} by considering $\theta = \pi/4$, i.e., $\hat{c}_{1,2} = (\hat{a}_1 \pm \hat{a}_2)/\sqrt{2}$. We have:

$$\begin{aligned} \mathcal{L}\hat{\rho} = & -i[\hat{H}_{c_1, c_2}, \hat{\rho}] + \sum_{k=1,2} \frac{\gamma_{c_k}(n_{\text{th}} + 1)}{2} \mathcal{D}[\hat{c}_k] \rho \\ & + \frac{\gamma_{c_k} n_{\text{th}}}{2} \mathcal{D}[\hat{c}_k^\dagger] \rho, \end{aligned} \quad (28)$$

where

$$\hat{H}_{c_1, c_2} = \sum_k \bar{\omega} \hat{c}_k^\dagger \hat{c}_k + \frac{\Delta}{2} (\hat{c}_1^\dagger \hat{c}_2 + \hat{c}_2^\dagger \hat{c}_1), \quad (29)$$

where $\gamma_{c_1, c_2} = \gamma \mp \gamma_{12}$. Hence, the model of the two incoherently coupled modes \hat{a}_1 and \hat{a}_2 becomes that of two dissipative coherently coupled modes \hat{c}_1 and \hat{c}_2 in the appropriate basis (see Appendix A) for a general form of the Liouvillian \mathcal{L} , under the transformation in Eq. (27).

The effective NHH \hat{H}_{eff} in Eq. (21), in a rotating reference frame $\bar{\omega}$, then reads

$$\hat{H}_{c_1, c_2}^{\text{eff}} = \frac{1}{2} \begin{pmatrix} -i\gamma_{c_1} & \Delta \\ \Delta & -i\gamma_{c_2} \end{pmatrix}. \quad (30)$$

This effective NHH in Eq. (30) now indicates that the supermodes \hat{c}_1 and \hat{c}_2 constitute a *passive* \mathcal{PT} -symmetric

system [1, 2, 21, 22]. Namely, if one applies a gauge transformation

$$\begin{pmatrix} \hat{c}'_1 \\ \hat{c}'_2 \end{pmatrix} = \exp\left(-\frac{\gamma}{2}t\right) \begin{pmatrix} \hat{c}_1 \\ \hat{c}_2 \end{pmatrix}, \quad (31)$$

the modified NHH in Eq. (30) then reads

$$\hat{H}_{c_1, c_2}^{\text{eff}} = \frac{1}{2} \begin{pmatrix} i\gamma_{12} & \Delta \\ \Delta & -i\gamma_{12} \end{pmatrix}. \quad (32)$$

This NHH $\hat{H}_{c_1, c_2}^{\text{eff}}$, in Eq. (32), commutes with the \mathcal{PT} operator, i.e.,

$$\left[\hat{H}_{c_1, c_2}^{\text{eff}}, \mathcal{PT}\right] = 0. \quad (33)$$

In other words, *the initial loss-loss dynamics* for the supermodes \hat{c}_1 and \hat{c}_2 *becomes equivalent to the balanced gain-loss evolution*, apart from the global decay rate $\gamma/2$.

3. Summary

To sum up, we have shown that, by applying appropriate unitary transformations to the anti- \mathcal{PT} -symmetric NHH in Eq. (5), one can readily discover a hidden \mathcal{PT} -symmetry of the NHH. As such, the EP in Eq. (26) is associated not only with the anti- \mathcal{PT} -symmetry but also with \mathcal{PT} -symmetry breaking of the NHH, induced by the same interplay between the frequency difference Δ and incoherent coupling rate γ_{12} .

Note that the exact (broken) anti- \mathcal{PT} -symmetric phase is accompanied by the broken (exact) \mathcal{PT} -symmetric phase. Indeed, the eigenfrequencies of the NHH are left unchanged under the unitary transformations in Eq. (27), but the action of the \mathcal{PT} and anti- \mathcal{PT} symmetry is opposite for the purely imaginary eigenfrequencies. Such coexistence of the opposite symmetric phases has already been pointed out in Refs. [73, 90]. We stress that the possibility to witness different symmetries of the system by considering different operators offers great flexibility to explore different dynamical regimes and various kinds of nontrivial light behavior in this system in the semi-classical regime [73–75]. Moreover, we have explained that one can witness not only the \mathcal{PT} and anti- \mathcal{PT} symmetries, but can also physically switch between them by transforming the system two-mode output fields with an additional tunable linear coupler, e.g., a tunable beam splitter in optical implementations of the general model discussed.

B. Liouvillian exceptional points of higher orders

As it has been already stressed in Sec. III, *an HEP of any order n implies an LEP of any higher order $m \geq n$* . Below, we study the second and third order LEPs, which arise due to the presence of a second-order HEP in the system under consideration.

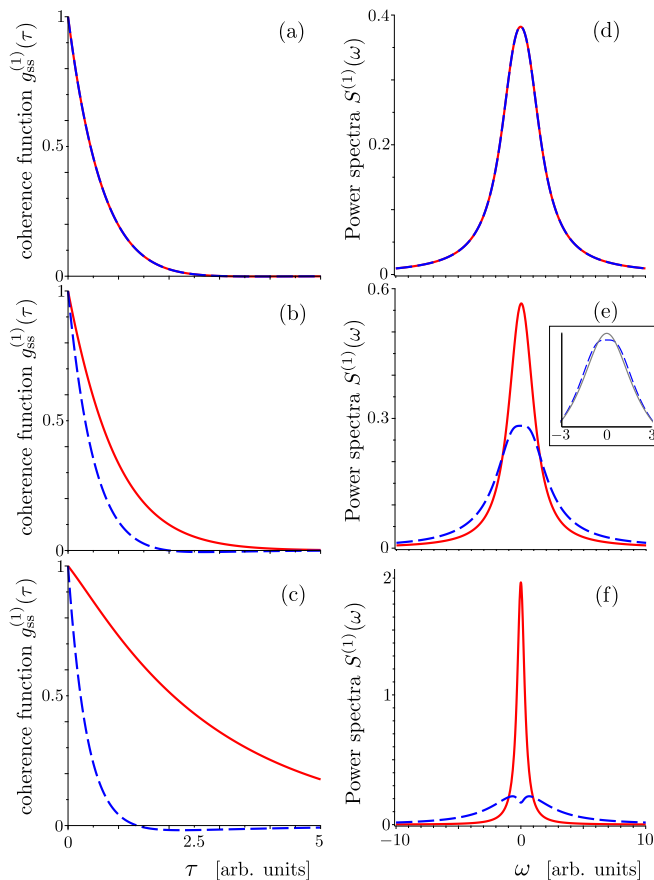


FIG. 2. First-order coherence function $g_{ss}^{(1)}(\tau)$ [panels (a)-(c)] and power spectra $S^{(1)}(\omega)$ [panels (d)-(f)] of the supermodes \hat{c}_1 (red solid curves) and \hat{c}_2 (blue dashed curves), according to Eqs. (35) and (36), respectively, of the bimodal cavity for various values of incoherent mode coupling rate γ_{12} : (a) [(d)] $\gamma_{12} = 0$ [arb. units]; (b) [(e)] $\gamma_{12} = \gamma_{12}^{\text{EP}1} = 1$ [arb. units]; and (c) [(f)] $\gamma_{12} = 2$ [arb. units]. The reference frame is rotating at the central cavity frequency $\bar{\omega}$. The remaining system parameters are the same as in Fig. 1. The spectra of the supermodes \hat{c}_1 and \hat{c}_2 reveal the squared Lorentzian lineshape at the second-order EP, characterized by a *plateau* at the top of the curve [see panel (e) blue dashed curve]. The inset in panel (e) shows the best Lorentzian fitting, represented by a sum of two Lorentzians (gray solid curve) of the spectrum at the EP (blue dashed curve), which highlights the distinctiveness of the squared Lorentzian. Thus, one can experimentally witness the presence of the EP by studying the power spectra for the model under consideration. Moreover, with increasing values of the incoherent mode-coupling rate $\gamma_{12} > \gamma_{12}^{\text{EP}1}$, the supermode \hat{c}_2 acquires a volcanic cone shape (blue dashed curve), indicating that its spectrum is represented by the difference of two Lorentzians [panel (f)].

1. LEP of second order and squared Lorentzian power spectra

The presence of an EP of second order in Eq. (26) can be signalled by a squared Lorentzian lineshape in the power spectrum of the \mathcal{PT} -symmetric modes $\hat{c}_{1,2}$ [29, 91–

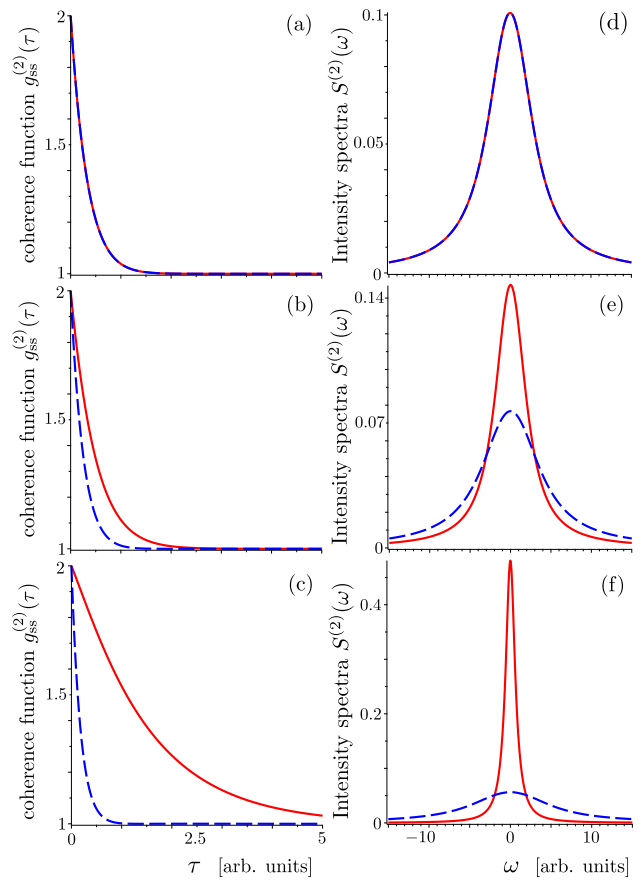


FIG. 3. Second-order coherence function $g_{ss}^{(2)}(\tau)$ [panels (a)-(c)] and intensity-fluctuation spectra $S^{(2)}(\omega)$ [panels (d)-(f)] of the supermodes \hat{c}_1 (red solid curves) and \hat{c}_2 (blue dashed curves), according to Eqs. (15) and (40), respectively, of the bimodal cavity for various values of incoherent mode coupling rate γ_{12} . The system parameters for each panel are the same as in Fig. 2.

93]. Indeed, the anti- \mathcal{PT} -symmetric modes $\hat{a}_{1,2}$ generate two independent spectra, which are not coupled. Thus, it is impossible to see spectral lines merging which are highlighted by a squared Lorentzian for these modes. However, the spectra of the \mathcal{PT} -symmetric supermodes $\hat{c}_{1,2}$ can demonstrate the modes coalescence effect, characterized by the appearance of a *plateau* at the top of the lineshape curve.

The power spectrum $S^{(1)}(\omega)$ can be expressed via the first-order coherence function $g_{ss}^{(1)}(\tau)$ as

$$S^{(1)}(\omega) = \frac{1}{\pi} \text{Re} \int_0^{\infty} g_{ss}^{(1)}(\tau) \exp(i\omega\tau) d\tau, \quad (34)$$

Mathematically, $S^{(1)}(\omega)$ is, thus, the Fourier transform of the coherence function $g_{ss}^{(1)}(\tau)$, and, roughly speaking, indicates the response of the system to the injection of one particle at a frequency ω .

The coherence function $g_{ss}^{(1)}(\tau)$, for the supermodes

$\hat{c}_{1,2}$, with the help of Eq. (11), is found as:

$$g_{\hat{c}_1, \hat{c}_2}^{(1)}(\tau) = \frac{\exp\left(-\frac{\gamma\tau}{2} - i\bar{\omega}\tau\right)}{D} \left(D \cosh \frac{D\tau}{2} \pm \gamma_{12} \sinh \frac{D\tau}{2} \right). \quad (35)$$

The incoherent power spectra of the supermodes $\hat{c}_{1,2}$, thus, take the form

$$S_{\hat{c}_1, \hat{c}_2}^{(1)}(\omega) = \frac{1}{\pi D} \left[\frac{K_+(D \mp \gamma_{12})}{\Omega^2 + K_+^2} + \frac{K_-(D \pm \gamma_{12})}{\Omega^2 + K_-^2} \right], \quad (36)$$

where $\Omega = \omega - \bar{\omega}$, and $K_{\pm} = (\gamma \pm D)/2$.

In Fig. 2, we plot both the coherence function $g_{\hat{c}_1, \hat{c}_2}^{(1)}(\tau)$ and power spectra $S_{\hat{c}_1, \hat{c}_2}^{(1)}(\omega)$ for the supermodes \hat{c}_1 and \hat{c}_2 . Away from an EP, the coherence functions (power spectra) are a combination of two exponents (Lorentzians) for both fields \hat{c}_1 and \hat{c}_2 . When $\gamma_{12} = 0$, the functions $g_{\hat{c}_1, \hat{c}_2}^{(1)}(\tau)$ and spectra $S_{\hat{c}_1, \hat{c}_2}^{(1)}(\omega)$ are identical, and the system is in the exact (broken) \mathcal{PT} (anti- \mathcal{PT}) symmetric phase of the NHH. But if the losses γ are sufficiently large, the two cavity resonances ω_1 and ω_2 might not be resolved [see Fig. 2(d)]. At the EP $\gamma_{12} = \gamma_{12}^{\text{EP}}$, the coherence functions attain a nonexponential form:

$$g_{\hat{c}_1, \hat{c}_2}^{(1)}(\tau) = \exp\left(-\frac{\gamma\tau}{2} - i\bar{\omega}\tau\right) \left(1 \pm \frac{\gamma_{12}\tau}{2}\right). \quad (37)$$

We note that distinguishing the exponential from non-exponential behavior could be hard in practice [see Fig. 2(b)]. On the other hand, at the EP, the two spectra become a combination of the Lorentzian and squared Lorentzian lineshapes [see Fig. 2(e)]. Indeed, the power spectra $S_{\hat{c}_1, \hat{c}_2}^{(1)}$ at the EP become:

$$S_{\hat{c}_1, \hat{c}_2}^{\text{EP}_1}(\omega) = \frac{1}{\pi} \frac{4}{\gamma^2 + 4\Omega^2} \left(\gamma \mp \gamma_{12} \pm \frac{2\gamma^2\gamma_{12}}{\gamma^2 + 4\Omega^2} \right), \quad (38)$$

where Ω is given in Eq. (36).

For larger values of $\gamma_{12} > \gamma_{12}^{\text{EP}}$, the first mode \hat{c}_1 experiences further amplification, whereas the second mode \hat{c}_2 encounters an increased damping. Notice also that the \hat{c}_2 mode, representing the difference of two Lorentzians, is no longer characterized by a single maximum for sufficiently large γ_{12} [see Fig. 2(c)]. The Lorentzian subtraction can lead to a substantial decrease of the spectral signal at the central cavity frequency $\bar{\omega}$, meaning that the energy is completely transferred from the mode \hat{c}_2 to \hat{c}_1 . The latter leads to the observation of electromagnetically induced absorption in the system [73]. Clearly, the presence of the incoherent mode coupling gives rise to a number of nontrivial phenomena in the system, which are related to both anti- \mathcal{PT} and \mathcal{PT} symmetric systems.

2. Liouvillian exceptional point of third order and cubic Lorentzian intensity-fluctuation spectra

According to Eq. (15), the second-order coherence function $g^{(2)}(\tau)$ at the steady state is determined by

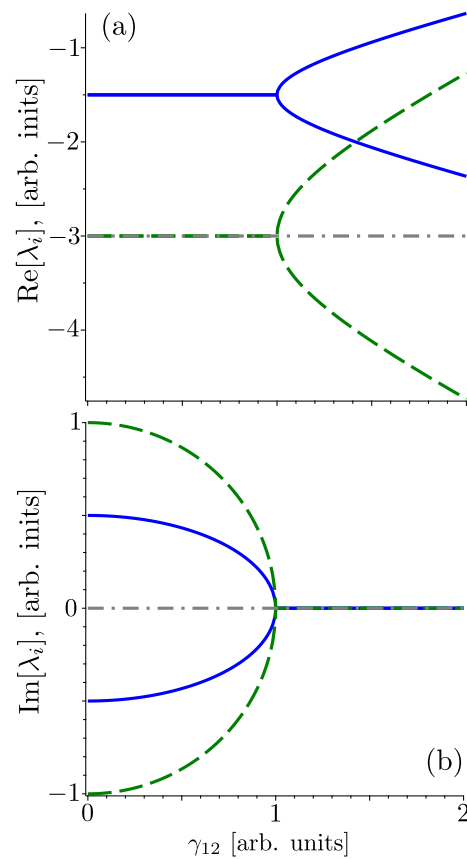


FIG. 4. (a) Real and (b) imaginary parts of the eigenvalues λ of the Liouvillian, determined from the evolution matrix \mathbf{M} : $\lambda_{1,2}$ (green dashed curves), and $\lambda_{3,4}$ (grey dash-dotted lines), according to Eq. (48), versus the incoherent coupling rate γ_{12} . The chosen system parameters are the same as in Fig. 1. For comparison, the Liouvillian eigenvalues defined by the NHH from Fig. 1 are shown as blue solid curves. Thus, for a given subspace of the Liouvillian eigenspace, determined by the NHH and evolution matrix M , the EP γ^{EP} , in Eq. (26), becomes a LEP of the second and third orders, respectively.

the coherence function $g^{(1)}(\tau)$. By exploiting Eqs. (15) and (35), one can arrive to an explicit expression for the function $g_{\hat{c}_1, \hat{c}_2}^{(2)}(\tau)$. Namely, at the EP in Eq. (26), from Eq. (37), one obtains

$$g_{\hat{c}_1, \hat{c}_2}^{(2)}(\tau) = 1 + \exp(-\gamma\tau) \left(1 \pm \frac{\gamma_{12}\tau}{2}\right)^2, \quad (39)$$

meaning that the function $g_{\hat{c}_1, \hat{c}_2}^{(2)}(\tau)$ signals the presence of a LEP of the third order. This third-order LEP is also reflected by the cubic Lorentzian lineshape in the intensity-fluctuation spectra, which is defined by the second-order coherence function $g^{(2)}(\tau)$ at the steady state as follows

$$S^{(2)}(\omega) = \frac{1}{\pi} \text{Re} \int_0^{\infty} \left[g^{(2)}(\tau) - 1 \right] \exp(i\omega\tau) d\tau. \quad (40)$$

By combining Eqs. (39) and (40), one easily arrives at the following expressions for the intensity-fluctuation spectra (or noise spectra) for the supermodes at the EP:

$$S_{\hat{c}_1, \hat{c}_2}^{(2)}(\omega) \equiv \frac{\gamma \mp \gamma_{12}}{\omega^2 + \gamma^2} - \frac{\gamma \gamma_{12} (3\gamma_{12} \mp 4\gamma)}{2(\omega^2 + \gamma^2)^2} + \frac{2\gamma^3 \gamma_{12}^2}{(\omega^2 + \gamma^2)^3}. \quad (41)$$

As predicted by Eq. (41), at the EP $\gamma = \gamma_{12}^{\text{EP}}$ of Eq. (26) the intensity-fluctuation spectra are cubic Lorentzians [see Figs. 3(d)-3(f)]. Experimentally, resolving the exact cubic lineshape might be challenging due to the simultaneous presence of the squared and cubic Lorentzians terms in Eq. (41). Thus, other techniques and methods might be required to precisely detect it [56]. As Fig. 3 shows, the intensity-fluctuations decrease (increase) for the mode \hat{c}_1 (\hat{c}_2), in accordance with the power spectra in Fig. 2.

3. Liouvillian exceptional point of third order explicitly defined from the higher-order field moments matrix

From Eqs. (35) and (15) one can even explicitly identify the Liouvillian eigenvalues, which determine the second-order coherence function $g^{(2)}(\tau)$, and the merging of which gives rise to third-order LEP. We have already shown in Fig. 3 how a third-order LEP gives rise to the cubic Lorentzian in the intensity-fluctuation spectra, along with a quadratic-time dynamics for the second-order coherence function $g^{(2)}(\tau)$ in Eq. (39). The system is $U(1)$ symmetric, that is, the Liouvillian is invariant under any phase shift ϕ of the boson operators $\hat{a}_j \rightarrow \hat{a}_j \exp(i\phi)$, $j = 1, 2$. Thus, the time dynamics of the coherence function $g^{(2)}(\tau)$ is completely determined by the second-order moments of the fields of the form $\langle \hat{a}_k^\dagger \hat{a}_l \rangle$, $k, l = 1, 2$. The dynamics of such moments is determined by the corresponding Liouvillian eigenspace. Therefore, the knowledge of the time evolution of the second-order moments $\langle \hat{a}_k^\dagger \hat{a}_l \rangle$ can reveal the presence of the third-order LEP.

The dynamics of the second-order moments can be described by the averages of $\hat{\mathbf{a}} = [(\hat{a}_1^\dagger, \hat{a}_2^\dagger) \otimes (\hat{a}_1, \hat{a}_2)]^T$. Indeed,

$$\frac{d}{dt} \langle \hat{\mathbf{a}} \rangle = \mathbf{M} \langle \hat{\mathbf{a}} \rangle + n_{\text{th}} \mathbf{b}. \quad (42)$$

The evolution matrix M for this vector of the averages $\langle \hat{\mathbf{a}} \rangle$ reads as

$$\mathbf{M} = \frac{1}{2} \begin{pmatrix} -2\gamma & -\gamma_{12} & -\gamma_{12} & 0 \\ -\gamma_{12} & 2i\Delta - 2\gamma & 0 & -\gamma_{12} \\ -\gamma_{12} & 0 & -2i\Delta - 2\gamma & -\gamma_{12} \\ 0 & -\gamma_{12} & -\gamma_{12} & -2\gamma \end{pmatrix}, \quad (43)$$

and the thermal noise vector is $\mathbf{b} = [\gamma, \gamma_{12}, \gamma_{12}, \gamma]^T$.

In the supermode basis, the evolution matrix \mathbf{N} and the noise vector \mathbf{d} for the vector $\hat{\mathbf{c}} = [(\hat{c}_1^\dagger, \hat{c}_2^\dagger) \otimes (\hat{c}_1, \hat{c}_2)]^T$ are easily found via the transformation

$$\mathbf{N} = \mathbf{T} \mathbf{M} \mathbf{T}^{-1}, \quad \mathbf{d} = \mathbf{T} \mathbf{b}, \quad (44)$$

where the 4×4 transformation matrix \mathbf{T} is given by

$$\mathbf{T} = \frac{1}{2} \begin{pmatrix} 1 & -1 \\ 1 & 1 \end{pmatrix} \otimes \begin{pmatrix} 1 & -1 \\ 1 & 1 \end{pmatrix}. \quad (45)$$

From Eqs. (42) and (44) it is evident that the dynamics for the vector of the averages $\langle \hat{\mathbf{a}} \rangle$ ($\langle \hat{\mathbf{c}} \rangle$) cannot, in general, possess anti- \mathcal{PT} (\mathcal{PT})-symmetry because of the presence of the thermal noise in the form of the vector \mathbf{b} (\mathbf{d}). Nevertheless, the matrix $i\mathbf{M}$ ($i\mathbf{N}$) is anti- \mathcal{PT} (\mathcal{PT})-symmetric. Indeed, the parity operator \mathcal{P} for the vector of the operators $\hat{\mathbf{a}}, \hat{\mathbf{c}}$ becomes

$$\mathcal{P} = \begin{pmatrix} 0 & 1 \\ 1 & 0 \end{pmatrix} \otimes \begin{pmatrix} 0 & 1 \\ 1 & 0 \end{pmatrix}. \quad (46)$$

With the help of Eq. (46) one can easily check that

$$\begin{aligned} \mathcal{PT}(i\mathbf{M})(\mathcal{PT})^{-1} &= -i\mathbf{M}, \\ \mathcal{PT}(i\mathbf{N}')(\mathcal{PT})^{-1} &= i\mathbf{N}', \end{aligned} \quad (47)$$

where the modified matrix \mathbf{N}' is obtained from \mathbf{N} by applying the gauge transformation in Eq. (31). The inclusion of the imaginary prefactor i in the matrices \mathbf{M} and \mathbf{N}' , in Eq. (47), ensures that the l.h.s. of the equations of motion for the vectors of the operators $\langle \hat{\mathbf{a}} \rangle$ and $\langle \hat{\mathbf{c}} \rangle$ remain unchanged under \mathcal{PT} transformation. Thus, in the absence of thermal photons $n_{\text{th}} = 0$, the dynamics for the averaged vector of operators $\langle \hat{\mathbf{a}} \rangle$ ($\langle \hat{\mathbf{c}} \rangle$) restores the same anti- \mathcal{PT} (\mathcal{PT})-symmetry imposed by the effective NHH on quantum fields in Eq. (21) [(30)]. As a result, the LEP of third order, determined from the evolution matrix \mathbf{M} (\mathbf{N}), becomes directly associated with anti- \mathcal{PT} (\mathcal{PT})-symmetry breaking.

The eigenvalues of the matrix \mathbf{M} , and thus of the matrix \mathbf{N} , are found as follows

$$\lambda_{1,2} = -2i\nu_{1,2}, \quad \lambda_{3,4} = -\gamma, \quad (48)$$

where $\nu_{1,2}$ are the eigenvalues of the NHH given in Eq. (23). We plot these eigenvalues in Fig. 4. At the EP γ_{12}^{EP} , the algebraic multiplicity of the eigenvalue $\lambda = -\gamma$ equals four, whereas geometric multiplicity is three. In other words, there is a coalescence of three Liouvillian eigenvectors, which are determined by the moments of the operators in the vectors $\hat{\mathbf{a}}$ and $\hat{\mathbf{c}}$, but the derivation of their explicit form might require other approaches [79, 94]. We also note that this finding of the LEP of third order for a second-order HEP in the space of the vector $\hat{\mathbf{c}}$ has already been observed in the single-photon regime for a similar system [56].

The presence of higher-order EPs in a system is usually associated with the enhanced system sensitivity to external perturbations in the vicinity of the EPs [1, 4]. This system's enhanced spectral response $\Delta\omega$ near an EP of an n th-order to a perturbation ϵ scales as $\Delta\omega \sim \epsilon^{\frac{1}{n}}$. Remarkably, the system spectral sensitivity around the LEP of the third-order can remain the same as it is near the second-order LEP. That is, the Liouvillian eigenvalues split near the third-order LEP, as $\Delta\lambda \sim \sqrt{\epsilon}$, not as

cubic root as one might expect. This squared-root dependence on perturbation around the third-order LEP arises from the system symmetry and the nature of the applied perturbation.

As it was explained earlier, the eigenvalues $\lambda_{1,2,3}$ Eq. (48) belong to the corresponding $U(1)$ Liouvillian eigenspace. As such, any perturbation of a single system parameter preserves the $U(1)$ symmetry of the system, e.g., $\gamma \rightarrow \gamma + \epsilon$. Consequently, the eigenvalue λ_3 (and the corresponding Liouvillian eigenmatrix) remain real (and Hermitian) under such a perturbation. Since λ_3 never acquires a imaginary part for such perturbations, only the complex eigenvalues $\lambda_{1,2}$, along with their eigenstates, induce a line splitting in the intensity-fluctuation spectrum around the third-order LEP. Thus, the spectral response to such external perturbations scales only as the squared root at the third-order LEP.

This result can be generalized to higher-order LEPs. Since any Liouvillian eigenvalue come in conjugate pairs, and given the \mathcal{PT} -symmetric structure of the system, given the coalescence of $(2k + 1)$ eigenvalues, one eigenvalue must always remain purely real in the vicinity of the LEP. Such an eigenvalue cannot contribute to the enhanced system spectral response under a perturbation. We conclude that, for the studied system, for any LEPs of odd order $(2k + 1)$, the system enhanced sensitivity scales at most as $\epsilon^{\frac{1}{2k}}$ around the LEP.

Finally, we would like to stress the mentioned difference in the dynamics of the higher-order field moments imposed by the Liouvillian and NHH. To show this explicitly we write the corresponding evolution matrix \mathbf{M}_{NHH} for the vector of the operators $\hat{\mathbf{a}}$, derived from the NHH in Eq. (21) as follows

$$\mathbf{M}_{\text{NHH}} = \frac{1}{2} \begin{pmatrix} 0 & \gamma_{12} & -\gamma_{12} & 0 \\ \gamma_{12} & 2i\Delta & 0 & -\gamma_{12} \\ -\gamma_{12} & 0 & -2i\Delta & \gamma_{12} \\ 0 & -\gamma_{12} & \gamma_{12} & 0 \end{pmatrix}. \quad (49)$$

A comparison of Eqs. (43) and (49) demonstrates that, indeed, the evolution imposed on the same operators is different in the Liouvillian and NHH formalisms. The eigenvalues of the matrix \mathbf{M}_{NHH} are similar to those in Eq. (48) but shifted by the value of γ , i.e., $\lambda_{\text{NHH}} = \lambda_{\mathcal{L}} + \gamma$, where $\lambda_{\mathcal{L}}$ are given in Eq. (48). Additionally, the inhomogeneous term \mathbf{b} , arising from the thermal noise, is absent in the equations of motion for the operators $\hat{\mathbf{a}}$ in the NHH formalism. Therefore, although the HEPs and LEPs can coincide for the same field moments, the system eigenspectra and dynamics are different in both formalisms [54, 56].

V. CONCLUSIONS

In this work, we have demonstrated that for a dissipative linear bosonic system, whose effective NHH exhibits a HEP of any finite order n , determined by the first-order field moments, its corresponding LEPs can become

at least of order $m \geq 2k(n - 1) + 1$, for $k = \frac{1}{2}, 1, 2, 3, \dots$, which can be determined by higher-order field moments, accordingly. These higher-order field moments are directly related to the *normally-ordered* higher-order coherence functions via the quantum regression theorem.

Thus, we have shown how the coherence functions can offer a convenient tool to probe extreme system sensitivity to external perturbations in the vicinity of higher-order LEPs.

As an example, we have studied a bosonic system of a bimodal cavity with incoherent mode coupling to reveal its higher-order LEPs. In particular, we analyze second and third-order LEPs of such systems arising from a HEP of second order by calculating the first- and second-order coherence functions, respectively. Also, we calculate the corresponding power and intensity-fluctuation spectra to reveal their squared and cubic Lorentzian expressions, accordingly. Moreover, our analysis of such two-mode systems indicates that, for the LEPs of an odd order $(2k + 1)$, the system enhanced sensitivity to external perturbations ϵ scales at most as $\epsilon^{\frac{1}{2k}}$.

We also reveal the anti- \mathcal{PT} - and \mathcal{PT} -symmetries of the NHH, which connect the presence of LEPs with spontaneous breaking of such symmetries in a bimodal cavity with incoherent mode coupling. Moreover, we showed the possibility of switching between the \mathcal{PT} and anti- \mathcal{PT} symmetries of the studied bosonic linear systems by applying an additional tunable linear coupler to two supermodes of the system output. By means of such coupler one can, thus, transform the initial loss-loss dynamics for the supermodes to the equivalent system with the balanced gain-loss evolution. In case of optical systems, this transformation can be implemented with a single tunable beam splitter.

We note that usually EPs have been studied in two- or multiparty systems with gain and loss (i.e., lossy driven systems). Here, we have analyzed EPs in a multiparty system without gain, but instead with its subsystems exhibiting losses with different rates. Such a system effectively leads to a model of a lossy-driven system.

In conclusion, we believe that our work has shown that the concept of quantum EPs, as defined via degeneracies of Liouvillians, is not only of a pure theoretical interest. We have demonstrated explicitly that the formalism of Ref. [54] can be tested experimentally at least for general quantum linear bosonic systems. In particular, LEPs can indeed be identified by measuring coherence functions or the power and intensity fluctuation spectra.

ACKNOWLEDGMENTS

I.A. thanks the Grant Agency of the Czech Republic (Project No. 18-08874S), and Project no. CZ.02.1.010.00.016_0190000754 of the Ministry of Education, Youth and Sports of the Czech Republic. A.M. is supported by the Polish National Science Centre (NCN) under the Maestro Grant No. DEC-

2019/34/A/ST2/00081. F.M. is supported by the FY2018 JSPS Postdoctoral Fellowship for Research in Japan. F.N. is supported in part by: NTT Research, Army Research Office (ARO) (Grant No. W911NF-18-1-0358), Japan Science and Technology Agency (JST) (via the CREST Grant No. JPMJCR1676), Japan Society for the Promotion of Science (JSPS) (via the KAKENHI Grant No. JP20H00134, and the JSPS-RFBR Grant No. JPJSBP120194828), and the Grant No. FQXi-IAF19-06 from the Foundational Questions Institute Fund (FQXi), a donor advised fund of the Silicon Valley Community Foundation.

Appendix A: Liouvillian \mathcal{L} for supermodes

Here we show an explicit form of the Liouvillian \mathcal{L} for the supermodes $\hat{c}_{1,2}$ in Eq. (27).

Considering a general Liouvillian, given in Eq. (2), for two modes with arbitrary damping matrix γ_{jk} and free Hermitian Hamiltonian in Eq. (20), after applying the transformations in Eq. (27), one arrives at the transformed master equation given by

$$\begin{aligned} \frac{d}{dt}\hat{\rho} = \mathcal{L}\hat{\rho} = & -i[\hat{H}_{c_1} + \hat{H}_{c_2} + \hat{H}_{c_1,c_2}, \hat{\rho}]\hat{\rho} \\ & + \mathcal{L}_{c_1}\hat{\rho} + \mathcal{L}_{c_2} + \mathcal{L}_{c_1,c_2}\hat{\rho} + \mathcal{L}_{c_2,c_1}\hat{\rho}, \end{aligned} \quad (\text{A1})$$

where the coherent part includes:

$$\begin{aligned} \hat{H}_{c_1} &= (\omega_1 \cos^2 \theta + \omega_2 \sin^2 \theta) \hat{c}_1^\dagger \hat{c}_1, \\ \hat{H}_{c_2} &= (\omega_1 \sin^2 \theta + \omega_2 \cos^2 \theta) \hat{c}_2^\dagger \hat{c}_2, \\ \hat{H}_{c_1,c_2} &= \frac{1}{2}(\omega_1 - \omega_2) \sin 2\theta (\hat{c}_1^\dagger \hat{c}_2 + \hat{c}_2^\dagger \hat{c}_1), \end{aligned} \quad (\text{A2})$$

and the incoherent Lindbladian part is:

$$\mathcal{L}_{c_m}\hat{\rho} = \frac{n_{\text{th}} + 1}{2} A_m \mathcal{D}[\hat{c}_m] + \frac{n_{\text{th}}}{2} A_m \mathcal{D}[\hat{c}_m^\dagger], \quad (\text{A3})$$

for $m = 1, 2$, and

$$\mathcal{L}_{c_j,c_k}\hat{\rho} = \frac{n_{\text{th}} + 1}{2} A_{jk} \mathcal{D}[\hat{c}_j \hat{c}_k^\dagger] + \frac{n_{\text{th}}}{2} A_{jk} \mathcal{D}[\hat{c}_j^\dagger \hat{c}_k], \quad (\text{A4})$$

with $j, k = 1, 2$ and $j \neq k$. Moreover we have denoted

$$\begin{aligned} A_1 &= \gamma_{11} \cos^2 \theta + \gamma_{22} \sin^2 \theta - \bar{\gamma}_{12} \sin 2\theta, \\ A_2 &= \gamma_{11} \sin^2 \theta + \gamma_{22} \cos^2 \theta + \bar{\gamma}_{12} \sin 2\theta, \\ A_{12} &= \gamma_- \sin 2\theta + \gamma_{12} \cos^2 \theta - \gamma_{21} \sin^2 \theta, \\ A_{21} &= \gamma_- \sin 2\theta + \gamma_{21} \cos^2 \theta - \gamma_{12} \sin^2 \theta. \end{aligned} \quad (\text{A5})$$

where $\bar{\gamma}_{12} = (\gamma_{12} + \gamma_{21})/2$, and $\gamma_- = (\gamma_{11} - \gamma_{22})/2$. Now, for the considered symmetric damping matrix ($\gamma_{11} = \gamma_{22}$ and $\gamma_{12} = \gamma_{21}$), by taking $\theta = \pi/4$, the Lindblad operators in Eq. (A1) become diagonalized. Thus, the initially lossy system with incoherent mode coupling becomes a lossy system with coherent mode coupling with an NHH, given in Eq. (30).

-
- [1] Ş. K. Özdemir, S. Rotter, F. Nori, and L. Yang, “Parity-time symmetry and exceptional points in photonics,” *Nature Materials* **18**, 783 (2019).
- [2] M. Miri and A. Alù, “Exceptional points in optics and photonics,” *Science* **363**, 7709 (2019).
- [3] Y. Ashida, Z. Gong, and M. Ueda, “Non-Hermitian physics,” (2020), [arXiv:2006.01837](https://arxiv.org/abs/2006.01837).
- [4] J. Wiersig, “Enhancing the sensitivity of frequency and energy splitting detection by using exceptional points: Application to microcavity sensors for single-particle detection,” *Phys. Rev. Lett.* **112**, 203901 (2014).
- [5] N. Zhang, S. Liu, K. Wang, Z. Gu, M. Li, N. Yi, S. Xiao, and Q. Song, “Single nanoparticle detection using far-field emission of photonic molecule around the exceptional point,” *Scientific Reports* **5**, 11912 (2015).
- [6] J. Wiersig, “Sensors operating at exceptional points: General theory,” *Phys. Rev. A* **93**, 033809 (2016).
- [7] J. Ren, H. Hodaei, G. Harari, A. U. Hassan, W. Chow, M. Soltani, D. Christodoulides, and M. Khajavikhan, “Ultrasensitive micro-scale parity-time-symmetric ring laser gyroscope,” *Optics Letters* **42**, 1556 (2017).
- [8] W. Chen, Ş. Kaya Özdemir, G. Zhao, J. Wiersig, and L. Yang, “Exceptional points enhance sensing in an optical microcavity,” *Nature (London)* **548**, 192–196 (2017).
- [9] H. Hodaei, A. U. Hassan, S. Wittek, H. Garcia-Gracia, R. El-Ganainy, D. N. Christodoulides, and M. Khajavikhan, “Enhanced sensitivity at higher-order exceptional points,” *Nature (London)* **548**, 187–191 (2017).
- [10] P.-Y. Chen, M. Sakhdari, M. Hajizadegan, Q. Cui, M. M.-C. Cheng, R. El-Ganainy, and A. Alù, “Generalized parity-time symmetry condition for enhanced sensor telemetry,” *Nature Electronics* **1**, 297–304 (2018).
- [11] Z.-P. Liu, J. Zhang, Ş. K. Özdemir, B. Peng, H. Jing, X.-Y. Lü, C.-W. Li, L. Yang, F. Nori, and Y.-X. Liu, “Metrology with \mathcal{PT} -symmetric cavities: Enhanced sensitivity near the \mathcal{PT} -phase transition,” *Phys. Rev. Lett.* **117**, 110802 (2016).
- [12] W. Langbein, “No exceptional precision of exceptional point sensors,” *Phys. Rev. A* **98**, 023805 (2018).
- [13] H.-K. Lau and A. A. Clerk, “Fundamental limits and non-reciprocal approaches in non-Hermitian quantum sensing,” *Nat. Commun.* **9**, 4320 (2018).
- [14] N. A. Mortensen, P. A. D. Gonçalves, M. Khajavikhan, D. N. Christodoulides, C. Tserkezis, and C. Wolff, “Fluctuations and noise-limited sensing near the exceptional point of parity-time-symmetric resonator systems,” *Op-*

- tica **5**, 1342 (2018).
- [15] M. Zhang, W. Sweeney, C. W. Hsu, L. Yang, A. D. Stone, and L. Jiang, “Quantum noise theory of exceptional point amplifying sensors,” *Phys. Rev. Lett.* **123**, 180501 (2019).
- [16] C. Chen, L. Jin, and R.-B. Liu, “Sensitivity of parameter estimation near the exceptional point of a non-Hermitian system,” *New J. Phys.* **21**, 083002 (2019).
- [17] H. Wang, Y.-H. Lai, Z. Yuan, M.-G. Suh, and K. Vahala, “Petermann-factor sensitivity limit near an exceptional point in a Brillouin ring laser gyroscope,” *Nat. Commun.* **11**, 1610 (2020).
- [18] J. Wiersig, “Prospects and fundamental limits in exceptional point-based sensing,” *Nat. Commun.* **11**, 2454 (2020).
- [19] T. Kato, *Perturbation theory for linear operators*, Classics in Mathematics (Springer, Berlin, 1995).
- [20] C. M. Bender and S. Boettcher, “Real spectra in non-Hermitian Hamiltonians having \mathcal{PT} symmetry,” *Phys. Rev. Lett.* **80**, 5243–5246 (1998).
- [21] L. Feng, R. El-Ganainy, and L. Ge, “Non-Hermitian photonics based on parity-time symmetry,” *Nat. Photon.* **11**, 752 (2017).
- [22] D. Christodoulides and J. Yang, eds., *Parity-time Symmetry and Its Applications* (Springer Singapore, 2018).
- [23] Z. Lin, H. Ramezani, T. Eichelkraut, T. Kottos, H. Cao, and D. N. Christodoulides, “Unidirectional invisibility induced by \mathcal{PT} -symmetric periodic structures,” *Phys. Rev. Lett.* **106**, 213901 (2011).
- [24] A. Regensburger, C. Bersch, M.-A. Miri, G. Onishchukov, D. N. Christodoulides, and U. Peschel, “Parity-time synthetic photonic lattices,” *Nature (London)* **488**, 167 (2012).
- [25] L. Feng, Z. J. Wong, R.-M. Ma, Y. Wang, and X. Zhang, “Single-mode laser by parity-time symmetry breaking,” *Science* **346**, 972 (2014).
- [26] H. Hodaei, M.-A. Miri, M. Heinrich, D. N. Christodoulides, and M. Khajavikhan, “Parity-time-symmetric microring lasers,” *Science* **346**, 975 (2014).
- [27] B. Peng, Ş. K. Özdemir, F. Lei, F. Monifi, M. Gianfreda, G. L. Long, S. Fan, F. Nori, C. Bender, and L. Yang, “Parity-time-symmetric whispering-gallery microcavities,” *Nat. Phys.* **10**, 394 (2014).
- [28] L. Chang, X. Jiang, S. Hua, C. Yang, J. Wen, L. Jiang, G. Li, G. Wang, and M. Xiao, “Parity-time symmetry and variable optical isolation in active-passive-coupled microresonators,” *Nat. Photon.* **8**, 524 (2014).
- [29] I. I. Arkhipov, A. Miranowicz, O. Di Stefano, R. Stassi, S. Savasta, F. Nori, and Ş. K. Özdemir, “Scully-Lamb quantum laser model for parity-time-symmetric whispering-gallery microcavities: Gain saturation effects and nonreciprocity,” *Phys. Rev. A* **99**, 053806 (2019).
- [30] H. Jing, Ş. K. Özdemir, X.-Y. Lü, J. Zhang, L. Yang, and F. Nori, “ \mathcal{PT} -symmetric phonon laser,” *Phys. Rev. Lett.* **113**, 053604 (2014).
- [31] H. Lü, Ş. K. Özdemir, L. M. Kuang, F. Nori, and H. Jing, “Exceptional points in random-defect phonon lasers,” *Phys. Rev. App.* **8**, 044020 (2017).
- [32] M. Brandstetter, M. Liertzer, C. Deutsch, P. Klang, J. Schoberl, H. E. Tureci, G. Strasser, K. Unterrainer, and S. Rotter, “Reversing the pump dependence of a laser at an exceptional point,” *Nat. Commun.* **5**, 4034 (2014).
- [33] B. Peng, Ş. K. Özdemir, S. Rotter, H. Yilmaz, M. Liertzer, F. Monifi, C. M. Bender, F. Nori, and L. Yang, “Loss-induced suppression and revival of lasing,” *Science* **346**, 328 (2014).
- [34] R. Huang, Ş. K. Özdemir, J. Q. Liao, F. Minganti, L. M. Kuang, Franco Nori, and H. Jing, “Exceptional photon blockade,” (2020), [arXiv:2001.09492](https://arxiv.org/abs/2001.09492).
- [35] J. Schindler, A. Li, M.C. Zheng, F. M. Ellis, and T. Kottos, “Experimental study of active LRC circuits with \mathcal{PT} symmetries,” *Phys. Rev. A* **84**, 040101(R) (2011).
- [36] H. Jing, Ş. K. Özdemir, Z. Geng, J. Zhang, X.-Y. Lü, B. Peng, L. Yang, and F. Nori, “Optomechanically-induced transparency in parity-time-symmetric microresonators,” *Scientific Reports* **5**, 9663 (2015).
- [37] H. Xu, D. Mason, L. Jiang, and J. G. E. Harris, “Topological energy transfer in an optomechanical system with exceptional points,” *Nature (London)* **537**, 80 (2016).
- [38] H. Jing, Ş. K. Özdemir, H. Lü, and F. Nori, “High-order exceptional points in optomechanics,” *Scientific Reports* **7**, 3386 (2017).
- [39] X. Zhu, H. Ramezani, C. Shi, J. Zhu, and X. Zhang, “ \mathcal{PT} -symmetric acoustics,” *Phys. Rev. X* **4**, 031042 (2014).
- [40] R. Fleury, D. Sounas, and A. Alù, “An invisible acoustic sensor based on parity-time symmetry,” *Nat. Commun.* **6**, 5905 (2015).
- [41] H. Benisty, A. Degiron, A. Lupu, A. De Lustrac, S. Chenais, S. Forget, M. Besbes, G. Barbillon, A. Bruyant, S. Blaize, and G. Lerondel, “Implementation of \mathcal{PT} symmetric devices using plasmonics: principle and applications,” *Optics Express* **19**, 18004 (2011).
- [42] M. Kang, F. Liu, and J. Li, “Effective spontaneous \mathcal{PT} -symmetry breaking in hybridized metamaterials,” *Phys. Rev. A* **87**, 053824 (2013).
- [43] D. Leykam, K. Y. Bliokh, C. Huang, Y. D. Chong, and F. Nori, “Edge modes, degeneracies, and topological numbers in non-Hermitian systems,” *Phys. Rev. Lett.* **118**, 040401 (2017).
- [44] J. González and R. A. Molina, “Topological protection from exceptional points in Weyl and nodal-line semimetals,” *Phys. Rev. B* **96**, 045437 (2017).
- [45] W. Hu, H. Wang, P. Ping Shum, and Y. D. Chong, “Exceptional points in a non-Hermitian topological pump,” *Phys. Rev. B* **95**, 184306 (2017).
- [46] T. Gao, G. Li, E. Estrecho, T. C. H. Liew, D. Comber-Todd, A. Nalitov, M. Steger, K. West, L. Pfeiffer, D. W. Snoke, A. V. Kavokin, A. G. Truscott, and E. A. Ostrovskaya, “Chiral modes at exceptional points in exciton-polariton quantum fluids,” *Phys. Rev. Lett.* **120**, 065301 (2018).
- [47] T. Liu, Y.-R. Zhang, Q. Ai, Z. Gong, K. Kawabata, M. Ueda, and F. Nori, “Second-order topological phases in non-Hermitian systems,” *Phys. Rev. Lett.* **122**, 076801 (2019).
- [48] L. Zhou, Q.-H. Wang, H. Wang, and J. Gong, “Dynamical quantum phase transitions in non-Hermitian lattices,” *Phys. Rev. A* **98**, 022129 (2018).
- [49] K. Y. Bliokh, D. I. Leykam, M. Lein, and F. Nori, “Topological non-Hermitian origin of surface Maxwell waves,” *Nature Communications* **10**, 580 (2019).
- [50] M. van Caspel, S. E. T. Arze, and I. P. Castillo, “Dynamical signatures of topological order in the driven-dissipative Kitaev chain,” *SciPost Phys.* **6**, 26 (2019).
- [51] Z.-Y. Ge, Y.-R. Zhang, T. Liu, S.-W. Li, H. Fan, and F. Nori, “Topological band theory for non-Hermitian systems from the Dirac equation,” *Phys. Rev. B* **100**, 054105 (2019).

- (2019).
- [52] J. Peřina and A. Lukš, “Quantum behavior of a \mathcal{PT} -symmetric two-mode system with cross-Kerr nonlinearity,” *Symmetry* **11**, 1020 (2019).
- [53] J. Peřina, A. Lukš, J. K. Kalaga, W. Leoński, and A. Miranowicz, “Nonclassical light at exceptional points of a quantum \mathcal{PT} -symmetric two-mode system,” *Phys. Rev. A* **100**, 053820 (2019).
- [54] F. Minganti, A. Miranowicz, R. W. Chhajlany, and F. Nori, “Quantum exceptional points of non-Hermitian Hamiltonians and Liouvillians: The effects of quantum jumps,” *Phys. Rev. A* **100**, 062131 (2019).
- [55] T. Prosen, “ \mathcal{PT} -symmetric quantum Liouvillean dynamics,” *Phys. Rev. Lett.* **109**, 090404 (2012).
- [56] I. I. Arkhipov, A. Miranowicz, F. Minganti, and F. Nori, “Quantum and semiclassical exceptional points of a linear system of coupled cavities with losses and gain within the Scully-Lamb laser theory,” *Phys. Rev. A* **101**, 013812 (2020).
- [57] F. Minganti, A. Miranowicz, R. W. Chhajlany, I. I. Arkhipov, and F. Nori, “Hybrid-Liouvillean formalism connecting exceptional points of non-Hermitian Hamiltonians and Liouvillians via postselection of quantum trajectories,” *Phys. Rev. A* **101**, 062112 (2020).
- [58] B. Jaramillo Ávila, C. Ventura-Velázquez, R. de J. León-Montiel, Y. N. Joglekar, and B. M. Rodríguez-Lara, “ \mathcal{PT} -symmetry from Lindblad dynamics in a linearized optomechanical system,” *Sci. Rep* **10**, 1761 (2020).
- [59] J. Huber, P. Kirton, S. Rotter, and P. Rabl, “Emergence of \mathcal{PT} -symmetry breaking in open quantum systems,” (2020), [arXiv:2003.02265](https://arxiv.org/abs/2003.02265).
- [60] A. Purkayastha, M. Kulkarni, and Y. N. Joglekar, “Emergent \mathcal{PT} symmetry in a double-quantum-dot circuit QED set-up,” (2020), [arXiv:2004.07541](https://arxiv.org/abs/2004.07541).
- [61] J. Wiersig, “Robustness of exceptional point-based sensors against parametric noise: The role of Hamiltonian and Liouvillian degeneracies,” *Phys. Rev. A* **101**, 053846 (2020).
- [62] D. Huybrechts, F. Minganti, F. Nori, M. Wouters, and N. Shammah, “Validity of mean-field theory in a dissipative critical system: Liouvillian gap, $\mathbb{P}\mathbb{T}$ -symmetric anti-gap, and permutational symmetry in the XYZ model,” *Phys. Rev. B* **101**, 214302 (2020).
- [63] G. Agarwal, *Quantum Optics* (Cambridge University Press, Cambridge, UK, 2013).
- [64] M. A. Quiroz-Juárez, A. Perez-Leija, K. Tschernig, B. M. Rodríguez-Lara, O. S. Magaña-Loaiza, K. Busch, Y. N. Joglekar, and R. de J. León-Montiel, “Exceptional points of any order in a single, lossy waveguide beam splitter by photon-number-resolved detection,” *Photon. Res.* **7**, 862 (2019).
- [65] S. M. Zhang, X. Z. Zhang, L. Jin, and Z. Song, “High-order exceptional points in supersymmetric arrays,” *Phys. Rev. A* **101**, 033820 (2020).
- [66] G. Hackenbroich, C. Viviescas, and F. Haake, “Quantum statistics of overlapping modes in open resonators,” *Phys. Rev. A* **68**, 063805 (2003).
- [67] S. Franke, S. Hughes, M. K. Dezfouli, P. T. Kristensen, K. Busch, A. Knorr, and M. Richter, “Quantization of quasinormal modes for open cavities and plasmonic cavity quantum electrodynamics,” *Phys. Rev. Lett.* **122**, 213901 (2019).
- [68] V. Eremin, S. E. Skipetrov, and M. Orszag, “Quantum theory of a two-mode open-cavity laser,” *Phys. Rev. A* **84**, 023816 (2011).
- [69] Ph. Grangier and J.-Ph. Poizat, “A simple quantum picture for the Petermann excess noise factor,” *Eur. Phys. J. D* **1**, 97 (1998).
- [70] H. A. M. Leymann, C. Hopfmann, F. Albert, A. Foerster, M. Khanbekyan, C. Schneider, S. Höfling, A. Forchel, M. Kamp, J. Wiersig, and S. Reitzenstein, “Intensity fluctuations in bimodal micropillar lasers enhanced by quantum-dot gain competition,” *Phys. Rev. A* **87**, 053819 (2013).
- [71] M. Fanaei, A. Foerster, H. A. M. Leymann, and J. Wiersig, “Effect of direct dissipative coupling of two competing modes on intensity fluctuations in a quantum-dot-microcavity laser,” *Phys. Rev. A* **94**, 043814 (2016).
- [72] N. P. Ong, W. Bauhofer, and C.-j. Wei, “Microwave Hall measurements in the intermediate conductivity regime using a bimodal cavity,” *Rev. Sci. Instrum.* **52**, 1367 (1981).
- [73] F. Zhang, Y. Feng, X. Chen, L. Ge, and W. Wan, “Synthetic anti- \mathcal{PT} symmetry in a single microcavity,” *Phys. Rev. Lett.* **124**, 053901 (2020).
- [74] H. Fan, J. Chen, Z. Zhao, J. Wen, and Y. Huang, “Antiparity-time symmetry in passive nanophotonics,” (2020), [arXiv:2003.11151](https://arxiv.org/abs/2003.11151).
- [75] Y. Li, Y.-G. Peng, L. Han, M.-A. Miri, W. Li, M. Xiao, X.-F. Zhu, J. Zhao, A. Alù, S. Fan, and Ch.-W. Qiu, “Anti-parity-time symmetry in diffusive systems,” *Science* **364**, 170 (2019).
- [76] Y. Choi, C. Hahn, J. W. Yoon, and S. H. Song, “Observation of an anti- \mathcal{PT} -symmetric exceptional point and energy-difference conserving dynamics in electrical circuit resonators,” *Nat. Commun.* **9**, 2182 (2018).
- [77] P. Peng, W. Cao, C. Shen, W. Qu, J. Wen, L. Jiang, and Y. Xiao, “Anti-parity-time symmetry with flying atoms,” *Nat. Phys.* **12**, 1139 (2016).
- [78] H. J. Carmichael, *Statistical Methods in Quantum Optics 1* (Springer, Berlin, 2010).
- [79] D. Honda, H. Nakazato, and M. Yoshida, “Spectral resolution of the Liouvillian of the Lindblad master equation for a harmonic oscillator,” *J. Math. Phys.* **51**, 072107 (2010).
- [80] F. Minganti, A. Biella, N. Bartolo, and C. Ciuti, “Spectral theory of Liouvillians for dissipative phase transitions,” *Phys. Rev. A* **98**, 042118 (2018).
- [81] T. Fink, A. Schade, S. Höfling, C. Schneider, and A. Imamoglu, “Signatures of a dissipative phase transition in photon correlation measurements,” *Nature Physics* **14**, 365–369 (2018).
- [82] N. Bartolo, F. Minganti, W. Casteels, and C. Ciuti, “Exact steady state of a Kerr resonator with one- and two-photon driving and dissipation: Controllable Wigner-function multimodality and dissipative phase transitions,” *Phys. Rev. A* **94**, 033841 (2016).
- [83] W. Casteels, R. Fazio, and C. Ciuti, “Critical dynamical properties of a first-order dissipative phase transition,” *Phys. Rev. A* **95**, 012128 (2017).
- [84] S. R. K. Rodriguez, W. Casteels, F. Storme, N. Carlon Zambon, I. Sagnes, L. Le Gratiet, E. Galopin, A. Lemaître, A. Amo, C. Ciuti, and J. Bloch, “Probing a dissipative phase transition via dynamical optical hysteresis,” *Phys. Rev. Lett.* **118**, 247402 (2017).
- [85] M. Fitzpatrick, N. M. Sundaresan, A. C. Y. Li, J. Koch, and A. A. Houck, “Observation of a dissipative phase transition in a one-dimensional circuit QED lattice,”

- [Phys. Rev. X **7**, 011016 \(2017\)](#).
- [86] M. Foss-Feig, P. Niroula, J. T. Young, M. Hafezi, A. V. Gorshkov, R. M. Wilson, and M. F. Maghrebi, “Emergent equilibrium in many-body optical bistability,” [Phys. Rev. A **95**, 043826 \(2017\)](#).
- [87] F. Vicentini, F. Minganti, R. Rota, G. Orso, and C. Ciuti, “Critical slowing down in driven-dissipative Bose-Hubbard lattices,” [Phys. Rev. A **97**, 013853 \(2018\)](#).
- [88] K. Svozil, “Squeezed fermion states,” [Phys. Rev. Lett. **65**, 3341–3343 \(1990\)](#).
- [89] L. Mandel and E. Wolf, *Optical Coherence and Quantum Optics* (Cambridge University Press, Cambridge, 1995).
- [90] L. Ge, “Symmetry-protected zero-mode laser with a tunable spatial profile,” [Phys. Rev. A **95**, 023812 \(2017\)](#).
- [91] G. Yoo, H.-S. Sim, and H. Schomerus, “Quantum noise and mode nonorthogonality in non-Hermitian \mathcal{PT} -symmetric optical resonators,” [Phys. Rev. A **84**, 063833 \(2011\)](#).
- [92] W. R. Sweeney, Ch. W. Hsu, S. Rotter, and A. D. Stone, “Perfectly absorbing exceptional points and chiral absorbers,” [Phys. Rev. Lett. **122**, 093901 \(2019\)](#).
- [93] A. Pick, B. Zhen, O. D. Miller, C. W. Hsu, F. Hernandez, A. W. Rodriguez, M. Soljačić, and S. G. Johnson, “General theory of spontaneous emission near exceptional points,” [Opt. Express **25**, 12325 \(2017\)](#).
- [94] L. Teuber and S. Scheel, “Solving the quantum master equation of coupled harmonic oscillators with Lie-algebra methods,” [Phys. Rev. A **101**, 042124 \(2020\)](#).